Electronic Supplementary Material (ESI) for Physical Chemistry Chemical Physics.

Electronic Supplementary Information for

Irreversible structural change of a dry ionic liquid under nanoconfinement

Andres Jurado[b], Hojun Kim[c], Andrea Arcifa [a], Antonella Rossi [a,d] , Cecilia Leal[c], Nicholas D. Spencer [a], and Rosa M. Espinosa-Marzal* [a,b]

[a]Lab. for Surface Science and Technology, Dept. of Materials, ETH Zurich, CH-8093 Zurich, Switzerland

[b]Dept. of Civil and Environmental Engineering, University of Illinois at Urbana-Champaign, IL-61801 Urbana, USA

[c]Dept. of Materials Science and Engineering, University of Illinois at Urbana-Champaign, IL-61801 Urbana, USA

[d]Dipartimento di Scienze Chimiche e Geologiche, Università di Cagliari, 09042 Cagliari, Italy.

	IL Layer Size in nm							
Approach	**A**	**B**	**C**	**D**	**E**	**F**	**G**	**H**
1st	5.1	1.3	-	-	-	-	-	-
5th	-	-	1.9	3.0	3.2	1.2	2.6	1.8
7th	-	-	1.9	4.3	3.0	3.5	4.1	-
11th	-	-	4.7	3.1	4.0	2.1	6.6	2.2

Table S1: Measured size of the layers resolved by colloidal-probe AFM for dry [HMIM] $EtSO_4$ on mica, at a lateral offset position ~50 μm from the initial confinement position. Force measurements were obtained under a N_2 atmosphere with a 40-μm-diameter colloidal probe at constant approach speeds of 20 nm s^{-1} (1st approach) and 15 nm s^{-1} (5th, 7th, and 11th approaches). Hertzian contact pressures did not exceed 31 MPa.

Force-distance measurements

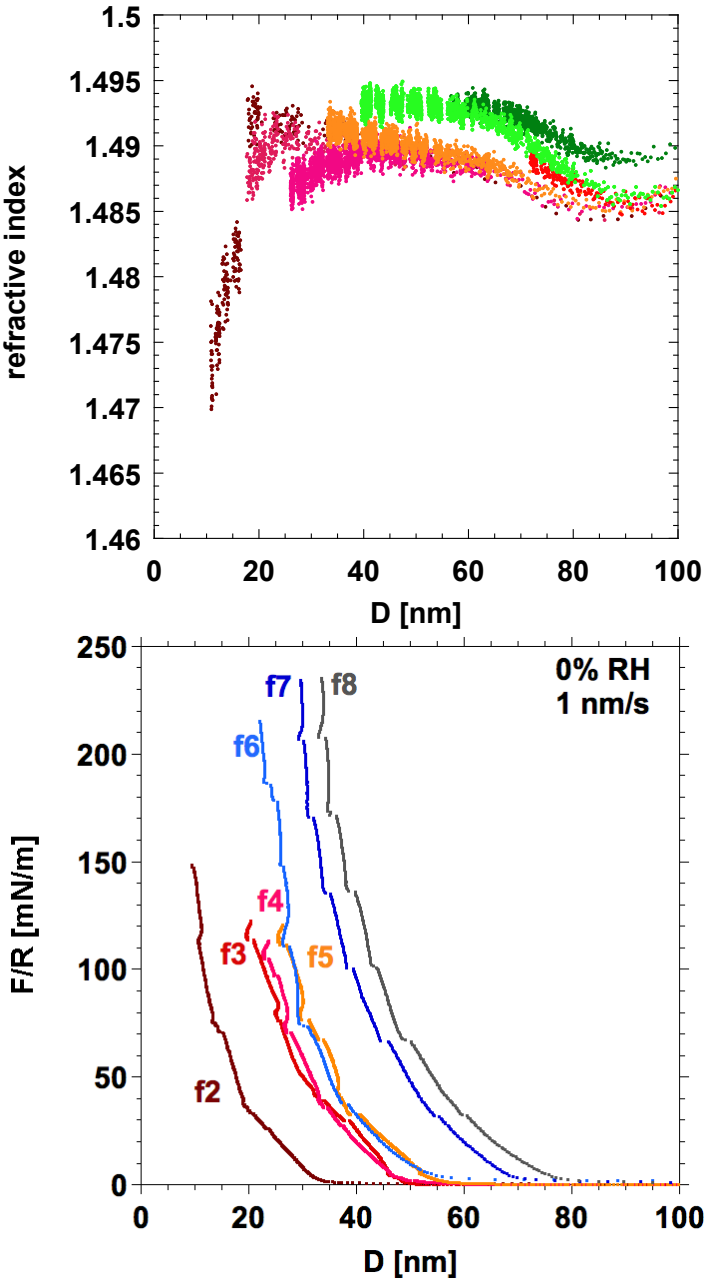

Figure S1: a) Measured refractive index during consecutive approaches. A discontinuity appears during a film-thickness transition. The variations are within the resolution of the measuring technique (±0.01 [-]). b) Force-distance curves of [HMIM] $EtSO_4$ in dry N_2 upon consecutive compression (from left to right) at 1 nm/s. The maximum applied load is smaller than 3 mN (150 mN/m) during the first 5 approaches and then it is increased to 4.6 mN. Although the results for different compressions are qualitatively in agreement, a systematic study of the effect of maximum load on the changes of the IL-structure in nanoconfinement is still required.

Dynamics of the film-thickness transitions

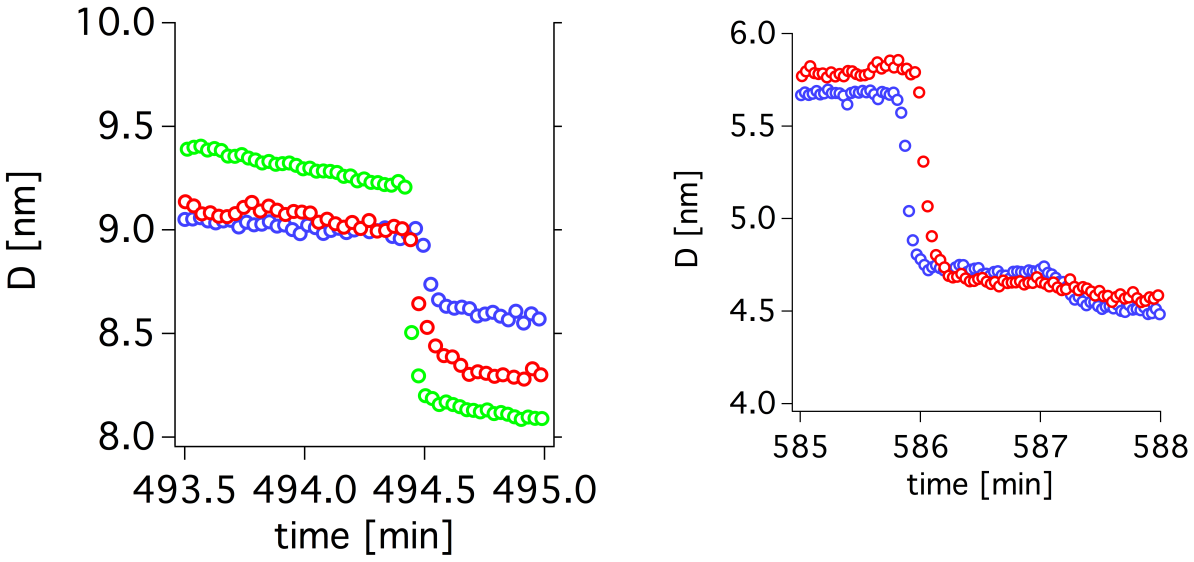

Figure S2: Dynamics of film-thickness transitions of [HMIM] $EtSO_4$ in dry N_2 during the first approach at 0.2 nm/s. Transitions on the right and left diagram were measured with different pairs of mica surfaces.

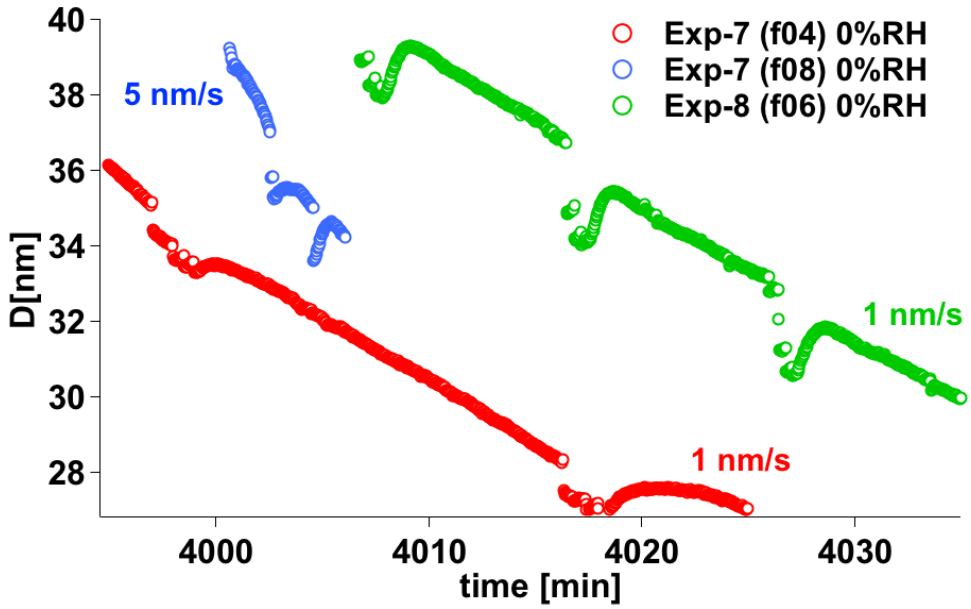

Figure S3: Dynamics of film-thickness transitions of [HMIM] $EtSO_4$ in dry N_2 (red circles). They consist of a rapid squeeze-out of layers (a) and a slow dilation (b). Transitions were measured with different pairs of mica surfaces (indicated by Exp-7 and Exp-8), and at 1 nm/s and 5 nm/s.

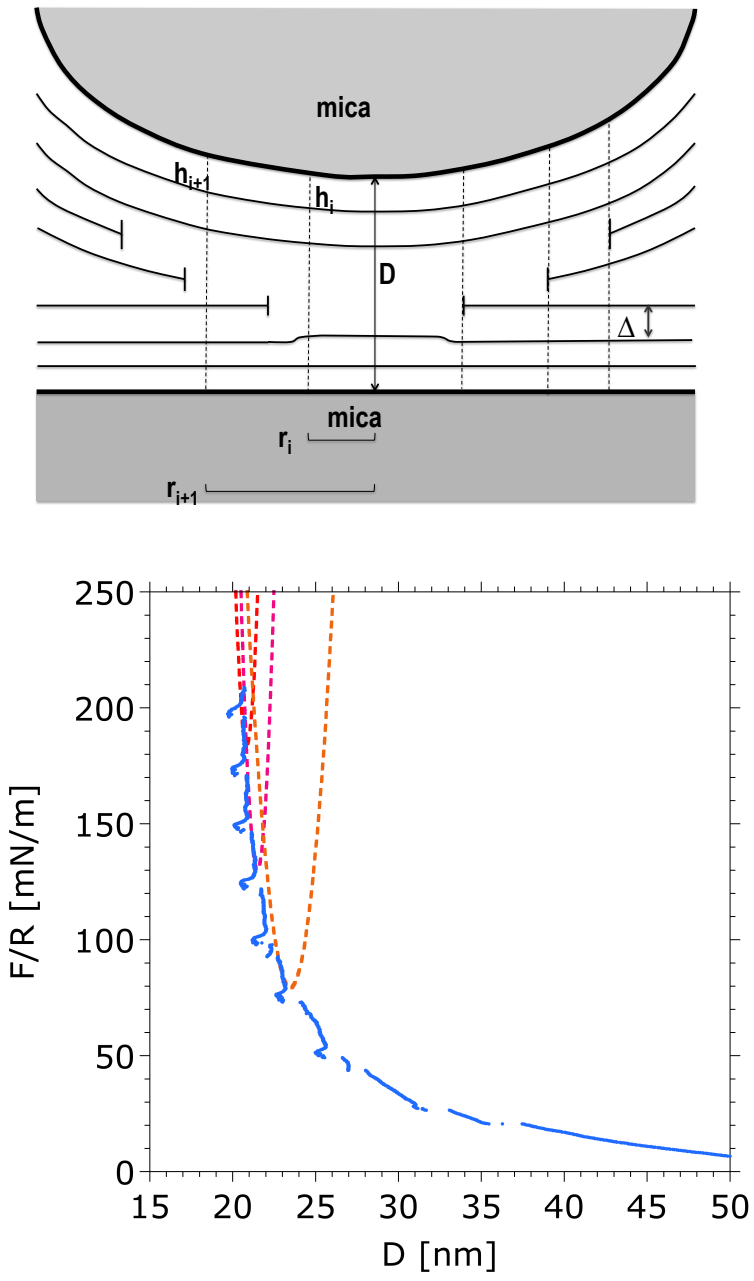

Figure S4: a) Contact-mechanics model for a layered film showing the central part that contributed to the stress and the toroidal cells containing a dislocation loop (adapted from ref. [1]). Such layered structures can relax the stress imposed by the curved confinement geometry by nucleating an array of concentric dislocation loops parallel to the plate and centered at the sphere-plate contact position. As the lateral distance from the center increases, the layers are progressively dilated until a dislocation loop is encountered. Here the structure discontinuously transitions from n_0 dilated layers to $n_0 + 1$ compressed layers. It can be shown that all toroidal cells containing a dislocation loop provide a negligible contribution to F, because they contain both compressed and dilated layers. Therefore, the only significant contribution to the force comes from the central stack of layers, located at the contact position, according to this model.

The contact region (and the stress) changes after each transition but this is not estimated with this model. b) Force-distance isotherm across [HMIM] $EtSO_4$ and fitted curves between film-thickness transitions.

Wide Angle X-ray Scattering (WAXS)

Dry ILs were transferred into 1.5 mm quartz X-ray capillaries (Hilgenberg Glas, Germany) in a glove box under dry conditions (flushed with N_2) and sealed with epoxy adhesive. The WAXS experiments were conducted in home-built (Forvis Technologies, Santa Barbara) equipment composed of a Xenocs GeniX3D CuK_α Ultra Low Divergence X-ray source (1.54Å / 8 keV), with a divergence of ~ 1.3 mrad. The sample-to-detector distance was 175.7 mm, yielding a q range of 0.86 nm^{-1} to 17.36 nm^{-1} (corresponding to 7.3–0.36 nm in real space). The 2D diffraction data were radially averaged upon acquisition on a Pilatus 300K 20 Hz hybrid pixel Detector (Dectris) and integrated using FIT2D software (http://www.esrf.eu/computing/scientific/FIT2D) from ESRF. The peak positions were determined after a Gaussian fit to the WAXS lines after a polynomial background reduction represented in Figure S14. The domain sizes are inversely proportional to the full width at half max (FWHM) of the WAXS line and, as can be observed in Figure S13, the ordered domains in [HMIM] $EtSO_4$ are twice as large as those observed with [HMIM]-Ntf2.

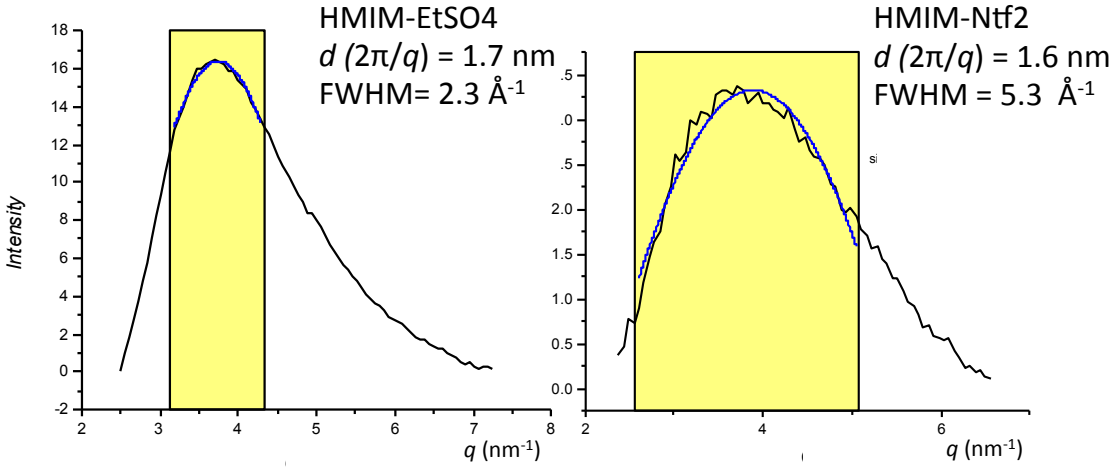

Figure S5: Gaussian fit to the low-q WAXS reflection (1st peak) obtained for [HMIM] $EtSO_4$ (left side) and [HMIM]-Ntf2 (right side). The fit was performed after a second-order-polynomial background reduction and yields the peak position - q (nm-1) and the width of the peak – FWHM. The peak position indicates the d spacing of the ordered domain and the FWHM is inversely proportional to the size of the ordered domain.

Force measurements with a sharp AFM tip

Sharp-tip AFM results show the short-range repulsive force with well-defined, superposed film-thickness transitions following repeated confinement, in agreement with other ILs. [2, 3] Figure S6 shows selected force isotherms for dry [HMIM] $EtSO_4$ on a freshly cleaved mica substrate in dry N_2 at a single position. Consecutive force isotherms are in excellent agreement. Two film-thickness transitions were observed, the largest being ~1.2 nm at ~0.5 nN, prior to the hard wall.

The layer thickness (~1.2 nm) is on the order of approximately twice the ion pair diameter. This suggests a self-assembled bilayer structure at the IL-solid interface, consistent with previous SFA measurements for other ionic liquids with long alkyl chains ([HMIM] Ntf2).[4] Results were reproducible across different positions and replicate experiments.

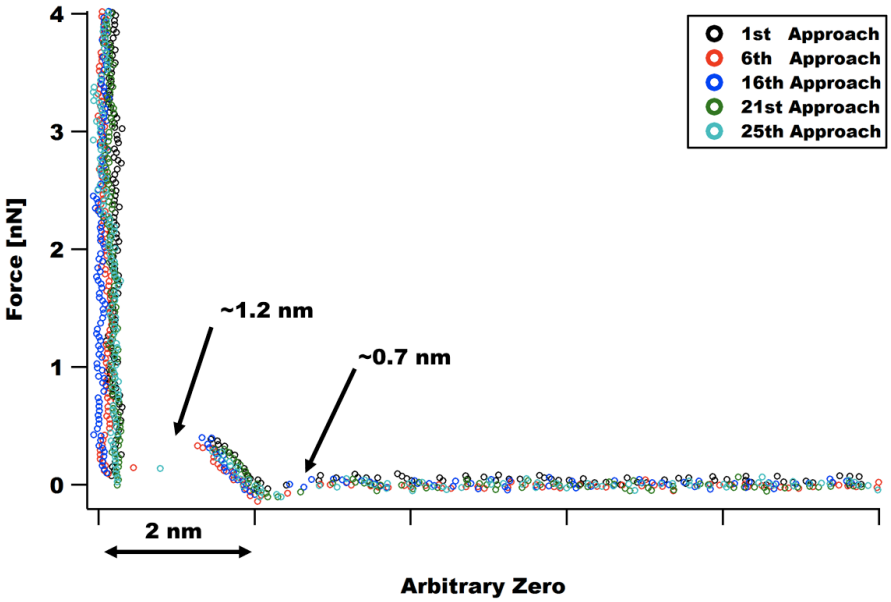

Figure S6: Force isotherms for dry [HMIM] $EtSO_4$ on a freshly cleaved mica surface in dry N_2 collected at a constant approach speed of 10 nm/s with a sharp (radius <12nm), silicon tip. Hertzian contact pressures did not exceed 6 GPa. Film-thickness transitions are indicated by the arrows.

Sharp-tip AFM results are in contrast to SFA and colloidal-probe AFM measurements, and are characterized by a *long-range* repulsion that gradually increases with consecutive approaches, and by multiple film-thickness transitions. The absence of these features suggests that a more pronounced confinement – i.e. a larger area of confinement - is required for [HMIM] $EtSO_4$ to undergo the reported liquid-to-solid phase transition. The small confinement area between the sharp tip and the substrate enables the intervening IL molecules to escape more easily.[5] Although Hertzian contact pressures are two orders-of-magnitude larger (same order of magnitude as the elastic modulus of the developed solid) than pressures achieved in SFA and colloidal-probe AFM experiments. The well-defined hard wall excludes a plastic deformation of the remaining solid-like IL-film at the surface.

Method: Sharp-tip AFM measurements were acquired with an Asylum Cypher (Santa Barbara, CA, USA) in contact mode. A gold coated, Si_3N_4 AFM cantilever with a sharp silicon tip ($r < 12$ nm) and spring constant of 0.24 N m-1 (Bruker, Camarillo, CA, USA) was used in this study. The spring constant of the AFM cantilever was determined according to the thermal-noise method.[6] The AFM tip was rinsed by immersing it in acetone for two hours, followed by isopropanol, and ethanol rinsing. Immediately before experiments the tip was treated in a UV-ozone cleaner for 20 minutes. Normal force-distance curves were obtained at approach speeds of 10 nm/s. The maximum applied force in the experiments reported here was 10 nN.

A 20 μL droplet of dry [HMIM] $EtSO_4$ was placed on a freshly cleaved mica surface. During the transfer, the droplet was exposed to ambient laboratory air (~35 % RH) for approximately two minutes, which might lead to traces of water in the IL. During the measurements, the AFM chamber was continuously purged with dry N_2. All force measurements were performed at RH < 2% and at 27 ± 2 ºC. The whole sequence of force measurements on a single mica piece was collected within 2 hours.

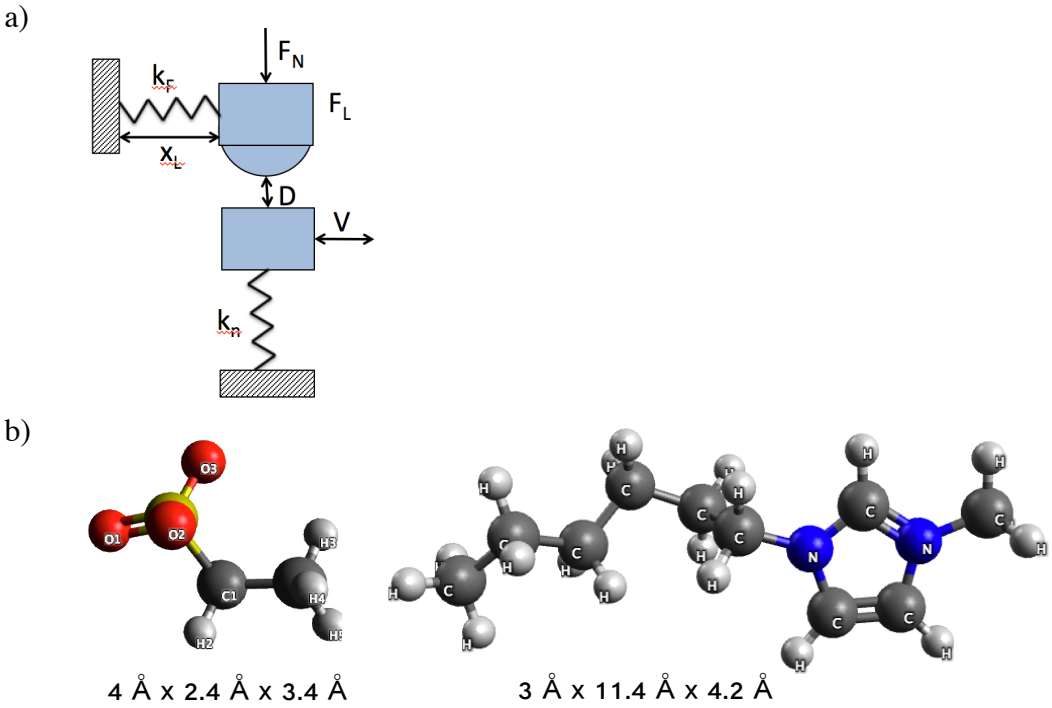

Figure S7: a) Schematics of the main features of the eSFA, indicating the two orthogonal springs k_n and k_f whose bending measures normal and shear forces between the surfaces as they are moved normally or laterally (x_L) to each other, respectively. B) Optimized geometry and size of HMIM+, and $EtSO_4$-, calculated with the software Avogadro by Molecular Mechanics (force field =MMFF94s).

X-ray photoelectron spectrum of [HMIM] $EtSO_4$

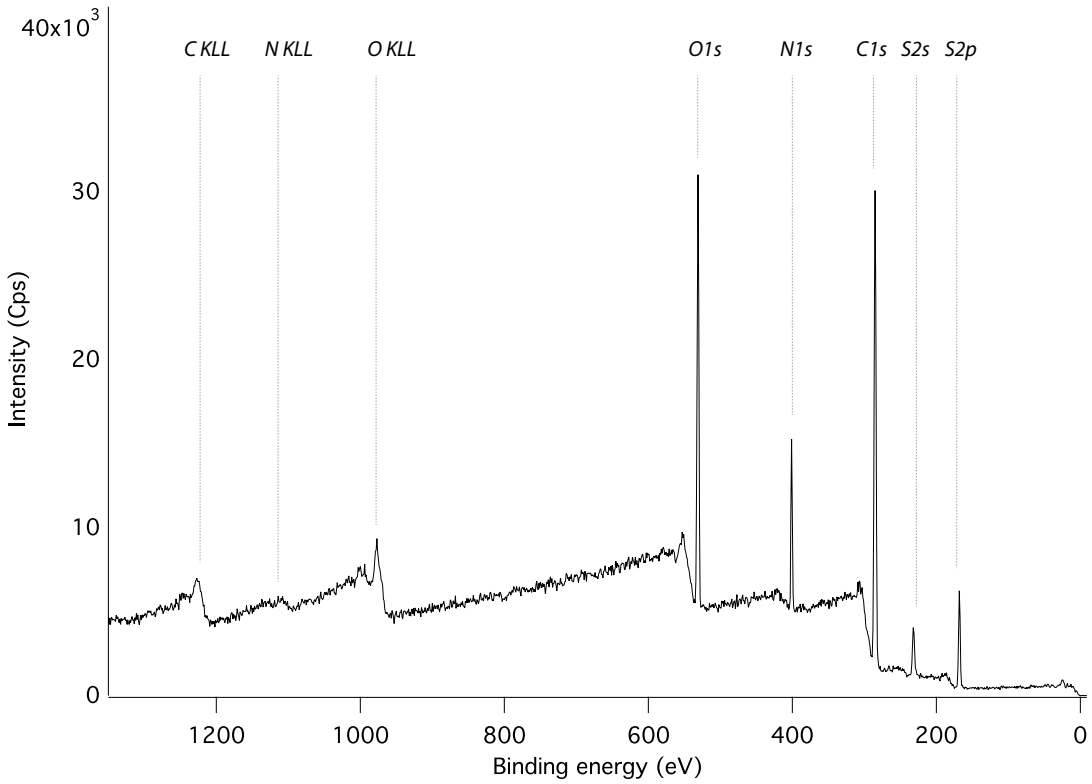

Figure S8: Survey spectra acquired acquired on a droplet of [HMIM] $EtSO_4$. The X-ray photoelectron spectra were acquired with a Theta Probe (Thermo Fisher Scientific, East Grinstead, U.K.). Droplets of the dry ionic liquid were deposited on mica surfaces and the spectra were measured on the droplet after 18 h in vacuum. Analyses were carried out with a monochromatic AlKα (1486.6 eV) source, using a beam diameter of 300 μm, the analyzer working in constant-analyzer-energy (CAE) mode. The survey spectra were acquired with a pass-energy of 300 eV and a step size of 1 eV. The acquisition time was 3 minutes and 45 seconds. The emission angle was 53°. The spectrometer was calibrated according to ISO 15472:2001 with an accuracy of ± 0.1 eV.

References

1. P. Richetti, P. Kekicheff and P. Barois, *J Phys Ii*, 1995, **5**, 1129-1154.

2. R. Hayes, S. Hayes, R. El Abedin and Atkin, *The journal of physical chemistry. B*, 2009, **113**, 7049-7052.

3. R. Atkin and G. G. Warr, *The Journal of Physical Chemistry C*, 2007, **111**, 5162-5168.

4. S. Perkin, L. Crowhurst, H. Niedermeyer, T. Welton, A. M. Smith and N. N. Gosvami, *Chemical Communications*, 2011, **47**, 6572-6574.

5. P. M. McGuiggan, J. Zhang and S. M. Hsu, *Tribology Letters*, 2001, **10**, 217-223.

6. J. L. Hutter and J. Bechhoefer, *Review of Scientific Instruments*, 1993, **64**, 1868-1873.